Recombinant *Listeria* promotes tumor rejection by CD8$^+$ T cell-dependent remodeling of the tumor microenvironment

Weiwen Deng[a,1], Victor Lira[a], Thomas E. Hudson[a], Edward E. Lemmens[a], William G. Hanson[a], Ruben Flores[a], Gonzalo Barajas[a], George E. Katibah[a], Anthony L. Desbien[a], Peter Lauer[a], Meredith L. Leong[a], Daniel A. Portnoy[b,c], and Thomas W. Dubensky Jr.[a,1,2]

[a]Aduro Biotech, Inc., Berkeley, CA 94710; [b]Department of Molecular and Cell Biology, University of California, Berkeley, CA 94720; and [c]The School of Public Health, University of California, Berkeley, CA 94720

Edited by Harvey Cantor, Dana-Farber Cancer Institute, Boston, MA, and approved June 29, 2018 (received for review February 6, 2018)

Agents that remodel the tumor microenvironment (TME), prime functional tumor-specific T cells, and block inhibitory signaling pathways are essential components of effective immunotherapy. We are evaluating live-attenuated, double-deleted *Listeria monocytogenes* expressing tumor antigens (LADD-Ag) in the clinic. Here we show in numerous mouse models that while treatment with nonrecombinant LADD induced some changes in the TME, no antitumor efficacy was observed, even when combined with immune checkpoint blockade. In contrast, LADD-Ag promoted tumor rejection by priming tumor-specific KLRG1$^+$PD1^{lo}CD62L$^-$ CD8$^+$ T cells. These IFNγ-producing effector CD8$^+$ T cells infiltrated the tumor and converted the tumor from an immunosuppressive to an inflamed microenvironment that was characterized by a decrease in regulatory T cells (Treg) levels, a proinflammatory cytokine milieu, and the shift of M2 macrophages to an inducible nitric oxide synthase (iNOS)$^+$CD206$^-$ M1 phenotype. Remarkably, these LADD-Ag–induced tumor-specific T cells persisted for more than 2 months after primary tumor challenge and rapidly controlled secondary tumor challenge. Our results indicate that the striking antitumor efficacy observed in mice with LADD-based immunotherapy stems from TME remodeling which is a direct consequence of eliciting potent, systemic tumor-specific CD8$^+$ T cells.

Listeria monocytogenes | CD8$^+$ T | tumor microenvironment | cancer vaccine

Under immunosuppressive tumor microenvironment (TME) conditions, tumor-specific T cells rapidly become exhausted (1). These dysfunctional T cells express high levels of inhibitory receptors (e.g., PD1, LAG3) and are impaired in their ability to produce cytokines such as TNFα and IFNγ (2). Suppressive leukocyte populations in the TME that inhibit T cell function include regulatory T cells (Tregs), myeloid-derived suppressor cells (MDSCs), and tumor-associated macrophages (TAMs) (1). TAMs have distinct functional types ranging from classically activated macrophages (M1) associated with acute inflammation and functional T cell immunity, to immunosuppressive macrophages (M2) associated with promoting tumor proliferation (3). Of those genes that define M2 macrophages, arginase 1 (Arg1) and mannose receptor (CD206) led to the concept of alternative activation of macrophages (4). IFNγ—known originally as a macrophage activating factor—plays a major role in skewing macrophages toward an M1 phenotype (5). Activated M1 macrophages respond with an oxidative burst via inducible nitric oxide synthase (iNOS), and directly kill tumor cells as well as produce cytokines that promote antitumor immunity (3). Multiple strategies are being developed to overcome immunosuppression to induce effective antitumor immunity (6).

One approach being evaluated clinically to induce antitumor immunity is antigen-expressing viruses and intracellular bacteria (7, 8). Upon challenge with intracellular microorganisms such as *Listeria monocytogenes* (Lm), the immune system rapidly mounts an innate inflammatory response characterized by MCP-1, IL-12p70, and IFNγ production which promotes priming of pathogen-specific T cell immunity (9). These Ag-specific CD8$^+$ T cells express several receptors including the killer cell lectin-like receptor G1 (KLRG1), which has been used as a surrogate marker for terminally differentiated short-lived effector CD8$^+$ T cells (10). However, a recent study showed that a population of CD8$^+$ T cells bearing markers associated with effector cells (KLRG1^{hi}CD27^{lo}T-bet^{hi}Eomes^{lo}) persisted to the memory phase and provided optimal control of wild-type (WT) Lm (11).

We are evaluating a live-attenuated Lm immunotherapy platform that lacks two virulence genes, the actin assembly-inducing protein (*actA*) and internalin B (*inlB*); Lm Δ*actA*/Δ*inlB* (LADD,

Significance

The development of therapeutic cancer vaccines using recombinant microorganisms has been pursued for many decades. However, the underlying mechanisms of therapeutic cancer vaccines remain unclear. Here we compare recombinant *Listeria*-based cancer vaccines to synthetic long peptide and adenovirus delivery systems for tumor antigens, and describe immunologic correlates of antitumor efficacy of *Listeria*-based cancer vaccines. Our results show that the profound antitumor efficacy requires tumor microenvironment (TME) remodeling that depends on tumor-specific CD8$^+$ T cells induced by live-attenuated double-deleted *Listeria monocytogenes* expressing cognate tumor antigens. Together, this work highlights the importance of cognate tumor antigen expression by cancer vaccines and pinpoints the relationship between induced tumor antigen-specific immunity and the TME.

Author contributions: W.D., M.L.L., and T.W.D. designed research; W.D., V.L., T.E.H., E.E.L., R.F., G.B., and A.L.D. performed research; W.G.H., P.L., and D.A.P. designed and constructed LADD strains; W.D., V.L., T.E.H., E.E.L., and G.E.K. analyzed data; and W.D. and T.W.D. wrote the paper.

Conflict of interest statement: W.D., V.L., T.E.H., E.E.L., W.G.H., R.F., G.B., G.E.K., A.L.D., P.L., M.L.L., and T.W.D. are current or former paid employees of Aduro Biotech, and hold stock in the company. D.A.P. was supported by National Institutes of Health Grants 1P01 AI063302 and 1R01 AI027655 and a Grant from Aduro Biotech (IVRI). D.A.P. has a consulting relationship with and a financial interest in Aduro Biotech, and both he and the company stand to benefit from the commercialization of the results of this research.

This article is a PNAS Direct Submission.

Data deposition: The raw sequence data reported in this manuscript have been deposited in the National Center for Biotechnology Information Sequence Read Archive (https://www.ncbi.nlm.nih.gov/) with accession nos. SRR7271231, SRR7271232, SRR7271229, SRR7271230, and SRR7271233.

[1]To whom correspondence may be addressed. Email: wdeng@aduro.com or tdubensky@tempesttx.com.

[2]Present address: Tempest Therapeutics, San Francisco, CA 94104.

This article contains supporting information online at www.pnas.org/lookup/suppl/doi:10.1073/pnas.1801910115/-/DCSupplemental.

Published online July 23, 2018.

live-attenuated double-deleted Lm). *actA* deletion prevents cell-to-cell spread and renders bacteria avirulent in a mouse listeriosis model (12). *inlB* deletion blocks infection via the hepatocyte growth factor receptor (13). LADD is rapidly cleared in mice without significant hepatocyte damage following i.v. administration, and is >1,000-fold attenuated relative to WT Lm (14). The immunologic potency of LADD is equivalent to WT Lm. Several LADD-based strains have been administered to more than 400 subjects, in multiple clinical studies in patients with advanced malignancies. Here, we sought to understand how treatment of tumor-bearing mice with LADD affects the TME, and hypothesized that antitumor efficacy of LADD-Ag was due to both tumor-specific $CD8^+$ T cell immunity and TME modulation by this population.

Results

LADD-Ag Administration Inhibits Tumor Growth in a $CD8^+$ T Cell-Dependent Manner. To test efficacy and dissect the mechanism of action of antitumor responses, we constructed a LADD strain that expresses AH1 (LADD-AH1). AH1 is a dominant H-$2L^d$-restricted $CD8^+$ T cell epitope derived from endogenous retroviral antigen gp70 (15). This antigen is expressed in both CT26 and 4T1 tumor cells (*SI Appendix*, Fig. S1*A*) (16), which allowed us to test LADD-AH1 efficacy in BALB/c mice bearing these tumors. A single i.v. injection of LADD-AH1 induced complete CT26 tumor rejection in six of eight mice (Fig. 1*A*); however, no reduction in tumor growth was observed with LADD treatment. Notably, i.v. injection of adenovirus-expressing AH1 (Ad-AH1) did not control CT26 tumor growth. Consistently, LADD-AH1 induced robust peripheral AH1 responses, whereas LADD and Ad-AH1 induced poor AH1 responses (Fig. 1*B*). Similarly, LADD-AH1 treatment inhibited 4T1 tumor growth (Fig. 1*C*). Tumor growth was not inhibited in LADD-treated mice, even when combined with PD-1 blockade (Fig. 1*C*). In contrast, LADD-AH1 combined with α-PD-1 resulted in complete 4T1 tumor eradication (Fig. 1*C*).

Tumor-specific $CD8^+$ T cells were critical for LADD-AH1 efficacy, as control of CT26 tumor growth was largely lost by $CD8^+$ T cell depletion (Fig. 1*D*), which also prevented peripheral AH1 responses (*SI Appendix*, Fig. S1*B*). In contrast, depletion of $CD4^+$ T cells did not impact LADD-AH1 efficacy (*SI Appendix*, Fig. S1*C*). An adoptive transfer experiment further confirmed this $CD8^+$ T cell requirement where splenic $CD8^+$ T cells from LADD-AH1-treated 4T1 tumor-bearing mice completely protected recipients against 4T1 tumor growth (Fig. 1*E*).

To test whether this striking antitumor efficacy could be observed in distinct genetic backgrounds, C57BL/6 mice were implanted with the human papillomavirus (HPV)16-derived-E7 expressing TC1 tumor, which works as a surrogate for human HPV16 tumors (17). C57BL/6 mice bearing TC1 tumors were treated with LADD expressing E7 (LADD-E7) or OVA (LADD-OVA). LADD-E7 but not LADD-OVA was efficacious in this model (Fig. 1*F*), consistent with increased peripheral E7 responses upon LADD-E7 immunization (Fig. 1*G*). Interestingly, LADD-E7 did not induce detectable E7 responses in naive mice, indicating that the TC1 tumor primed tumor-specific immunity (Fig. 1*G*). In contrast, the Lm-specific listeriolysin O (LLO) responses were comparable in LADD-E7-treated tumor-bearing and naive mice (Fig. 1*G*). Of note, s.c. injection of E7 SLP formulated with AddaVax failed to control TC1 tumor growth (Fig. 1*H*), which is consistent with poor induction of E7 responses (*SI Appendix*, Fig. S1*D*). In line with our observations in BALB/c tumor models, $CD8^+$ T cell but not NK cell depletion prevented TC1 tumor control by LADD-E7 (*SI Appendix*, Fig. S1*E*). Together, these data demonstrated that LADD-induced antitumor efficacy requires expression of a relevant tumor antigen from LADD and $CD8^+$ T cells are essential for LADD-Ag potency.

LADD-Ag Immunotherapy Induces Splenic Tumor-Specific $CD8^+$ Effector T Cells. To determine whether Ag expression by LADD affected the cytokine profile, we measured serum cytokines induced by LADD and LADD-AH1 in CT26 tumor-bearing mice. At 6-h postinjection, LADD and LADD-AH1 induced comparable proinflammatory cytokines including MCP-1, IL-12p70 and IFNγ, demonstrating that Ag expression does not alter cytokines induction (*SI Appendix*, Fig. S2*A*). To assess possible functional differences, we performed RNA-Seq analysis of peripheral $CD8^+$ T cells purified from CT26 tumor-bearing mice that were treated with LADD or LADD-AH1. Principal component analysis indicated that peripheral $CD8^+$ T cells from HBSS, LADD, or LADD-AH1–treated mice exhibited distinct transcriptional features (*SI Appendix*, Fig. S2*B*). Remarkably, peripheral $CD8^+$ T cells from LADD-AH1–treated mice exhibited increased expression of genes related to

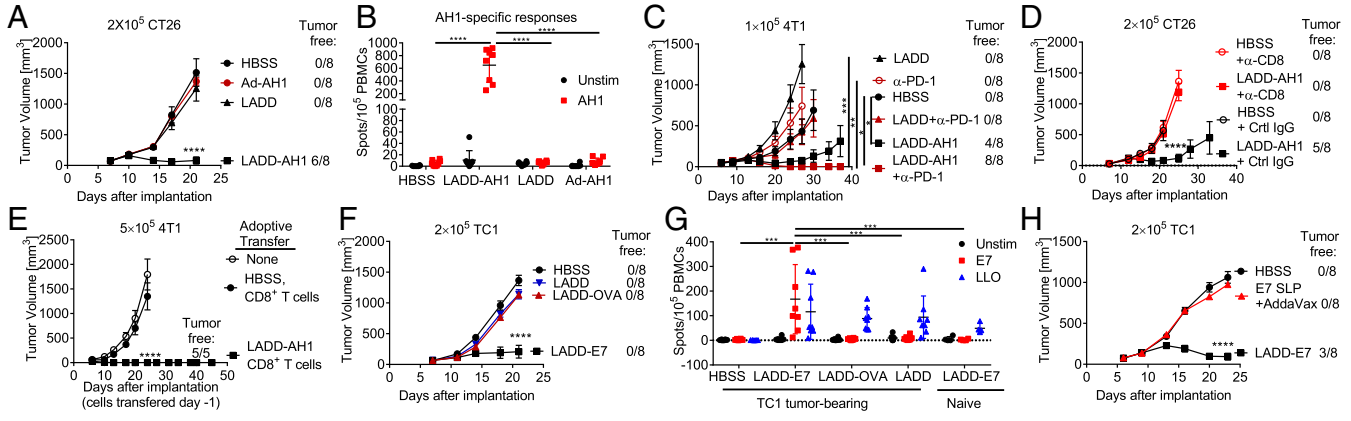

Fig. 1. LADD-Ag administration inhibits growth of multiple tumor models in a $CD8^+$ T cell-dependent manner. (*A*) S.c. growth of 2×10^5 CT26 in BALB/c mice ($n = 8$) i.v. injected with HBSS, 1×10^6 cfu LADD, LADD-AH1, or 1×10^7 CFU Ad-AH1 on day 7. (*B*) Peripheral blood mononuclear cell (PBMC) IFNγ ELISpot in *A* with AH1 peptide stimulation was performed on day 14. (*C*) S.c. growth of 1×10^5 4T1 in BALB/c mice ($n = 8$) treated with HBSS, LADD, or LADD-AH1 on Day 7. On Days 10 and 17, 100 μg α-PD1 was administered i.p. (*D*) S.c. growth of 2×10^5 CT26 tumor in BALB/c mice ($n = 8$) treated with HBSS or LADD-AH1 on day 7. On days 6 and 8, 200 μg control IgG or α-CD8 was administered i.p. (*E*) S.c. growth of 5×10^5 4T1 tumor in BALB/c mice ($n = 5$) which received splenic $CD8^+$ T cells of LADD-AH1 treated or control 4T1 tumor-bearing mice. (*F*) S.c. growth of 2×10^5 TC1 tumor in C57/BL6 mice ($n = 8$) i.v. injected with HBSS, LADD, LADD-OVA, or LADD-E7 on day 7. (*G*) PBMC IFNγ ELISpot in *F* were performed on day 14 with E7 or LLO peptide stimulation. (*H*) S.c. growth of 2×10^5 TC1 tumor in C57BL/6 mice ($n = 8$) i.v. injected with HBSS, LADD-E7, or s.c. injected with 100 μg E7 SLP formulated with AddaVax on day 7. Tumor volumes ±SEM are shown. Numbers of tumor-free mice are indicated in the figures. In scatter plots, each circle represents one mouse. *A*, *C*–*F*, and *H* were analyzed by two-way analysis of variance (ANOVA), and *B* and *G* were analyzed by Mann–Whitney *U* tests. $*P < 0.05$, $**P < 0.01$, $***P < 0.001$, and $****P < 0.0001$. Results are representative of at least two independent experiments.

T cell activation and cytotoxicity signatures, including a substantial increase in expression of *Tbx21*, *Ifng*, *Gzmb*, *Cx3cr1*, and *Klrg1*, relative to HBSS and LADD treatment (Fig. 2*A* and *SI Appendix*, Table S1). The magnitude of the peripheral AH1-specific $CD8^+$ T cell population also increased dramatically after LADD-AH1 treatment relative to LADD (Fig. 2*B*). This T cell population largely displayed a short-lived effector phenotype, characterized by $CD44^+CD62L^-KLRG1^+$, consistent with RNA-Seq analysis (Fig. 2 *C* and *D*). While $CD44^+CD62L^-$ $CD8^+$ T cells trended higher with LADD treatment relative to HBSS control mice, this difference was not significant (Fig. 2*C*). Notably, most of AH1-specific $CD8^+$ T cells induced by LADD-AH1 were $KLRG1^+CD62L^-CX_3CR1^+CD44^+$ (*SI Appendix*, Fig. S2 *C–F*).

Recent results from two clinical trials highlight the potential of targeting tumor-specific neoantigens with a therapeutic vaccine (18, 19). To test whether LADD can elicit neoantigen-specific $CD8^+$ T cells, we constructed an LADD strain expressing MC38 neoepitopes Adpgk and Reps1 (LADD-Neo) (20). Robust $Adpgk^+$ $CD8^+$ T cells were detected by tetramer staining in MC38 tumor-bearing mice treated with LADD-Neo (*SI Appendix*, Fig. S3 *A* and *B*). Significantly, most of the LADD-Neo-induced $Adpgk^+$ $CD8^+$ T cells were also $KLRG1^+$(*SI Appendix*, Fig. S3*B*). LADD-Neo induced significant responses against the Adpgk neoepitope but did not cross-react against its native sequence, and LADD-Neo induced higher Adpgk responses in tumor-bearing mice than in naive mice (*SI Appendix*, Fig. S3*C*).

To identify locations of tumor-specific $CD8^+$ T cell priming, immune responses in tumor draining lymph nodes (TDLN) and spleen were measured 4 d after LADD-AH1 treatment. TDLN cells from LADD-AH1–treated mice exhibited enhanced AH1 responses relative to those from HBSS or LADD treatment (Fig. 2*E*). Additionally, AH1 responses were observed in tumor-bearing but not naive mice, indicating that implanted CT26 cells primed AH1-specific responses (Fig. 2*E*). The splenic AH1 $CD8^+$ T cell response induced by LADD-AH1 was significantly higher than the response measured in the TDLN, which we confirmed by AH1 tetramer analysis (Fig. 2 *E* and *F*). These results indicated that AH1-specific $CD8^+$ T cells localized preferentially to the spleen and did not reside in the TDLN, likely due to a lack of CD62L expression (*SI Appendix*, Fig. S2*D*). Consistent with their predominant splenic localization, LADD-AH1-induced splenic $CD8^+$ T cells displayed increased Ki67, a proliferation marker (Fig. 2*G*). Furthermore, splenic $AH1^+CD8^+$ T cells induced by LADD-AH1 in CT26 tumor-bearing mice produced IFNγ in response to CT26 as well as 4T1 cells stimulation ex vivo (Fig. 2*H* and *SI Appendix*, Fig. S4 *A* and *B*). This was not surprising as both CT26 and 4T1 express Gp70 (*SI Appendix*, Fig. S1*A*). However, LADD-AH1 treatment failed to induce responses against CT26 neoepitopes whose vaccination were reported to reject CT26 tumor (21) (*SI Appendix*, Fig. S4*C*). However, these data do not exclude the possibility of epitope spreading upon LADD-Ag to unknown CT26 antigens.

Notably, splenic $AH1^+KLRG1^+$ $CD8^+$ T cells were strongly induced by LADD-AH1 treatment, whereas these cells existed at low levels in LADD and HBSS groups (Fig. 2*I*). To explore whether $AH1^+KLRG1^+$ $CD8^+$ T cells were differentiated and expanded from $AH1^+KLRG1^-$ $CD8^+$ T cells primed by tumor implantation, splenic $CD45.1^+CD8^+$ T cells from tumor-bearing mice were adoptively transferred into naive $CD45.2^+$ recipients. Indeed, donor $AH1^+KLRG1^-$ $CD8^+$ T cells expanded and differentiated into $AH1^+KLRG1^+$ $CD8^+$ T cells upon LADD-AH1 but not LADD immunization (Fig. 2*J* and *SI Appendix*, Fig. S4*D*). While an increase in KLRG1 expression and proliferation of donor $CD8^+$ T cells was observed in recipients upon LADD immunization, this strain did not expand $AH1^+$ $CD8^+$ T cells, demonstrating a requirement for LADD-mediated expression of the cognate tumor Ag (*SI Appendix*, Fig. S4*D*). Recipient $CD45.2^+AH1^+CD8^+$ T cells were detectable but at a low frequency following LADD-AH1 injection (Fig. 2*J*), consistent with a weak tumor-specific response in naive animals (Fig. 1*G* and *SI Appendix*, Fig. S3*C*).

LADD-Induced Functional Tumor-Specific $CD8^+$ T Cells Infiltrate into Tumors. TME modification to promote tumor cell destruction in malignancies is an essential step for effective immunotherapy. We measured the magnitude and interrogated the phenotype of $CD8^+$ T cells infiltrating CT26 tumors to characterize how LADD impacts the TME, and to determine whether LADD-induced tumor-specific $CD8^+$ T cells affected the TME profile. Immunohistochemistry (IHC) and flow cytometry analysis 4 d after LADD-AH1 treatment showed a marked increase in the frequency of tumor

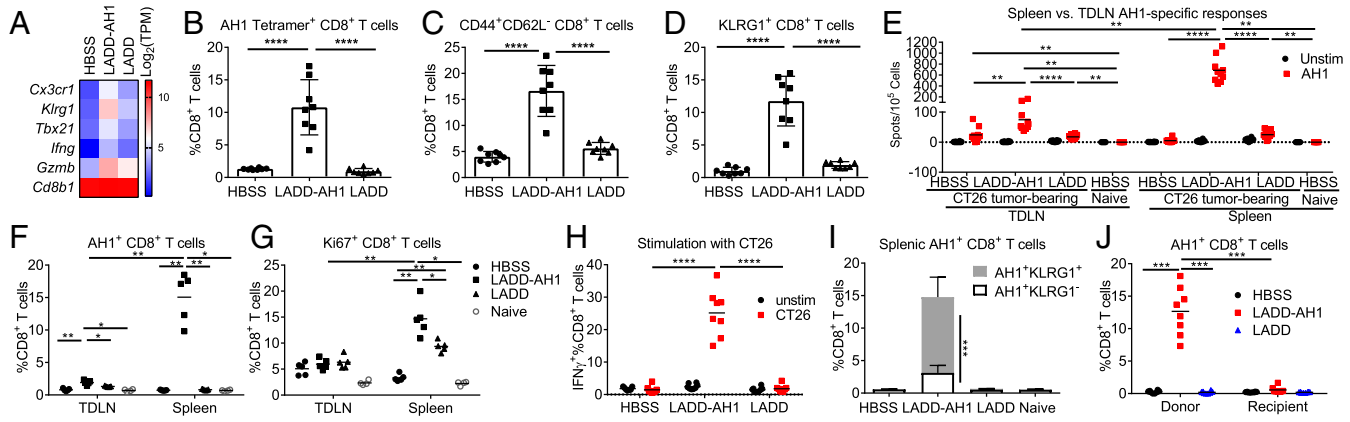

Fig. 2. LADD-AH1 immunotherapy induces splenic AH1-specific $CD8^+$ effector T cells. (*A–I*) CT26 tumor-bearing BALB/c mice ($n = 8$) were i.v. injected with HBSS, LADD, or LADD-AH1 on day 7. (*A–D*) On day 14, (*A*) RNA-Seq analysis of peripheral $CD8^+$ T cells purified from a pool of eight mice per group. Heat map of selected genes from the core signature. Log_2 of gene expression values (TPM, transcripts per million) are colored from blue to red. Frequencies of (*B*) AH1 $tetramer^+$, (*C*) $CD44^+CD62L^-$, and (*D*) $KLRG1^+$ of peripheral $CD8^+$ T cells were measured by flow staining. (*E–I*) On Day 11, (*E*) TDLN and spleen IFNγ ELISpot were performed with AH1 peptide stimulation. Naive mice served as control. (*F* and *G*) Frequency of (*F*) AH1 $tetramer^+$ and (*G*) $Ki67^+$ of TDLN or splenic $CD8^+$ T cells. (*H*) IFNγ production by splenic $CD8^+$ T cells were tested with CT26 cells stimulation ex vivo. (*I*) Frequency of $AH1^+KLRG1^-$ and $AH1^+KLRG1^+$ of splenic $CD8^+$ T cells. (*J*) Adoptive transfer of purified $CD45.1^+$ $CD8^+$ donor T cells from CT26 tumor-bearing mice into $CD45.2^+$ mice (recipients, $n = 8$). Mice were immunized with HBSS, LADD-AH1, and LADD one day later. Seven days postimmunization, frequency of AH1 $tetramer^+$ of donor and recipient $CD8^+$ T cells. *B–D* were analyzed by one-way ANOVA with Tukey's multiple comparisons test, *E–J* were analyzed by Mann–Whitney *U* tests. $^*P < 0.05$, $^{**}P < 0.01$, $^{***}P < 0.001$, and $^{****}P < 0.0001$. Results are representative of at least two independent experiments.

infiltrating CD8$^+$ T cells (Fig. 3 *A* and *B* and *SI Appendix*, Fig. S5*A*). Interestingly, PD-1 expression on CD8$^+$ T cells decreased with both LADD and LADD-AH1 treatment (Fig. 3*C*). Remarkably, treatment with LADD-AH1 but not LADD led to a massive increase in IFNγ-producing AH1-specific CD8$^+$ T cells in the TME (Fig. 3 *D* and *E*). Furthermore, the principal increased population of AH1$^+$ CD8$^+$ T cells in the TME induced by LADD-AH1 treatment were AH1$^+$KLRG1$^+$ CD8$^+$ effector cells (Fig. 3*F* and *SI Appendix*, Fig. S5*B*). RNA-Seq analysis revealed distinct gene signatures between the AH1$^+$KLRG1$^-$ and AH1$^+$KLRG1$^+$ CD8$^+$ T cell populations in LADD-AH1–treated tumors (Fig. 3*G*). AH1$^+$KLRG1$^+$CD8$^+$ T cells expressed higher levels of *Gzma*, *Ifng*, and *Ccl5*, but lower levels of *Pdcd1, Lag3, Ctla4, and Socs3* compared with AH1$^+$KLRG1$^-$CD8$^+$ T cells (Fig. 3*G* and *SI Appendix*, Table S2). Flow analysis confirmed that AH1$^+$KLRG1$^+$CD8$^+$ T cells expressed lower levels of PD-1, LAG3 (Fig. 3*H* and *SI Appendix*, Fig. S5 *C* and *D*) and produced higher levels of IFNγ (Fig. 3*I*), indicating that LADD-AH1 induced a functional AH1$^+$KLRG1$^+$ CD8$^+$ T cell population that was not exhausted.

To test AH1$^+$KLRG1$^+$ CD8$^+$ T cells primed in the spleen that subsequently trafficked into the TME, we used the sphingosine 1-phosphate analog FTY720, a drug that inhibits egress of lymphocytes including CD8$^+$ T cells from secondary lymphoid organs (22). While similar levels of AH1$^+$CD8$^+$ T cells were present in the TME of HBSS- or FTY720-treated mice, tumor-infiltrating AH1$^+$CD8$^+$ T cells were reduced in LADD-AH1–treated mice that also received FTY720 (Fig. 3*J*). Together, these results indicate that while the LADD itself induced changes in the TME, only LADD-AH1 induced IFNγ-producing AH1$^+$KLRG1$^+$ CD8$^+$ effector T cells that traffic to tumors.

TME Remodeling Is Dependent on LADD-Induced Tumor-Specific CD8$^+$ T Cells. The TME is highly immunosuppressive partially due to inhibitory cell populations, including Tregs, MDSCs, and TAMs. We next characterized these populations in the TME after LADD treatment. LADD-AH1 treatment decreased tumor-infiltrating Treg frequency (Fig. 4*A*), which when combined with the high magnitude of CD8$^+$ effector T cells in the TME (Fig. 3 *A* and *B*) dramatically increased the ratio of CD8$^+$ T cells to Tregs (CD8/Treg) ($P < 0.0001$; Fig. 4*B*). Interestingly, LADD treatment also decreased Treg frequency (Fig. 4*A*) and increased CD8/Treg ratio ($P < 0.05$) (Fig. 4*B*), consistent with TME modification by the LADD vector itself.

Interestingly, treatment with LADD-AH1 but not LADD induced iNOS production and prevented CD206 expression by TAMs, and this phenotype was completely abrogated by CD8$^+$ T cell depletion (Fig. 4 *C* and *D*). These results indicate that the tumoral M2 to M1 macrophage shift depended on LADD-AH1–induced CD8$^+$ T cells. TAM reprogramming following Lm phagocytosis has been previously reported (23). This is unlikely given that LADD-AH1 was enriched in the spleen and liver, but not the CT26 tumors of mice (Fig. 4*E*), and LADD was unable to induce TAM reprogramming. LADD-AH1 was cleared 7 d postinjection, when CT26 tumors started collapsing (*SI Appendix*, Fig. S6*A*). The discrepancy between our observation and previous reports may be due to difference in models.

To test whether CD8$^+$ T cells could directly mediate TAMs repolarization, we cocultured splenic CD8$^+$ T cells with an untreated CT26 tumor suspension ex vivo. Indeed, the presence of LADD-AH1–induced AH1$^+$CD8$^+$ effector T cells increased iNOS production and decreased CD206 expression in TAMs (Fig. 4 *F* and *G*). Increased iNOS production was blocked by α-IFNγ, while CD206 expression was unaffected (Fig. 4 *F* and *G*). These data suggested that IFNγ produced by AH1$^+$CD8$^+$ T cells is essential for iNOS production but not CD206 down-regulation.

To further test the role of TAMs in vivo, we employed anti-CSF-1R and anti-CCL2 antibodies to prevent TAMs recruitment into the tumor (24, 25). Anti-CSF-1R/CCL2 treatment delayed CT26 tumor growth, which might be a result of M2 removal from the TME (*SI Appendix*, Fig. S6*B*). Furthermore, LADD-AH1 still controlled CT26 tumor growth following anti-CSF-1R/CCL2 treatment although we observed a tendency toward increased tumor burden in some LADD-AH1–treated mice. These data suggest that TAMs are not essential for LADD-Ag efficacy.

We further examined the TME cytokine and chemokine profile by luminex. Consistent with TAMs repolarization, inflammatory cytokines including IFNγ and TNFα dramatically increased in the TME upon LADD-AH1 immunization (Fig. 4 *H* and *I*), which depended on LADD-AH1–induced CD8$^+$ T cells.

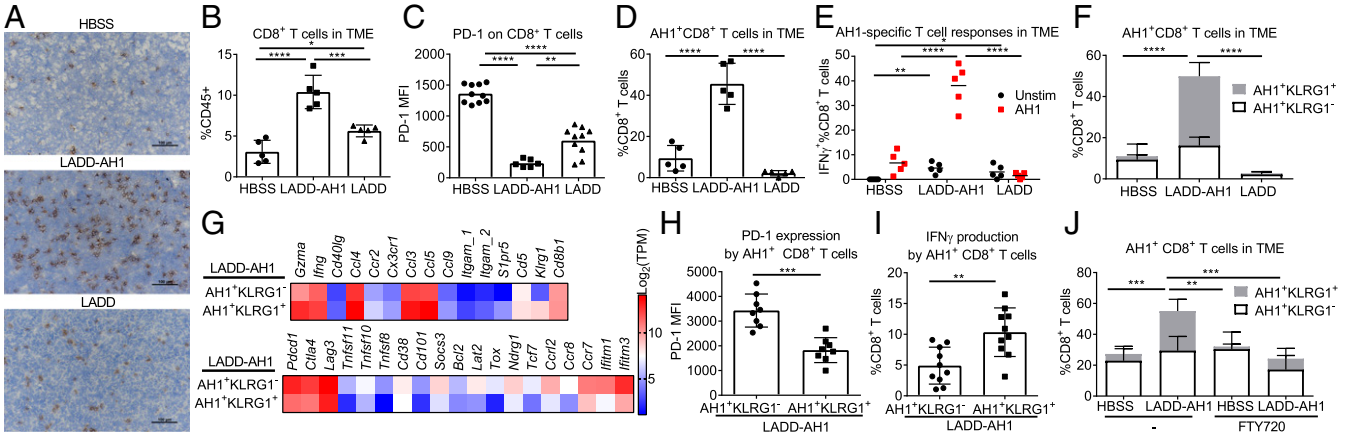

Fig. 3. Functional AH1-specific CD8$^+$ effector T cells induced by LADD-AH1 infiltrated CT26 tumors. CT26 tumor-bearing mice (n = 5–10) were immunized with HBSS, LADD-AH1, or LADD on day 7. (*A*) IHC staining of CD8$^+$ T cells infiltration of CT26 tumor on day 11. (Scale bars: 100 μm.) (*B*) Frequencies of CD8$^+$ T cells in CD45$^+$ population of the TME. (*C*) PD-1 expression on tumor-infiltrating CD8$^+$ T cells by calculation of mean fluorescence intensity (MFI). (*D*) Frequency of AH1 tetramer$^+$ of CD8$^+$ T cells. (*E*) Intracellular IFNγ production by tumor-infiltrating CD8$^+$ T cells were tested with AH1 peptide stimulation ex vivo. (*F*) Frequency of AH1$^+$KLRG1$^-$ and AH1$^+$KLRG1$^+$ of CD8$^+$ T cells. (*G–I*) Comparison of AH1$^+$KLRG1$^-$ and AH1$^+$KLRG1$^+$ tumor-infiltrating CD8$^+$ T cells from LADD-AH1–treated mice, (*G*) RNA-Seq analysis. Heat map of selected genes out of core signature. Log_2TPM are colored from blue to red. (*H*) PD-1 expression (MFI). (*I*) Intracellular IFNγ production. (*J*) Frequency of AH1$^+$KLRG1$^-$ and AH1$^+$KLRG1$^+$ of CD8$^+$ T cells in TME with or without FTY720 treatment. In scatter plots, each circle represents one mouse. *B–F* and *J* were analyzed by one-way ANOVA with Tukey's multiple comparisons test. *H* and *I* were analyzed by Mann–Whitney *U* tests. *$P < 0.05$, **$P < 0.01$, ***$P < 0.001$, and ****$P < 0.0001$.

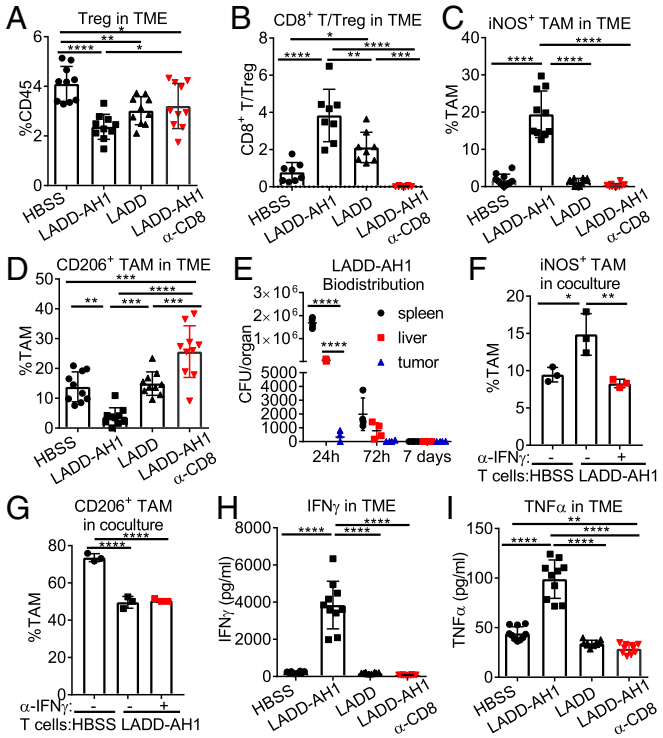

Fig. 4. Remodeling of TME is dependent on LADD-AH1–induced AH1-specific $CD8^+$ T cells. (*A–D*) CT26 tumor-bearing mice (n = 8–10) were immunized with HBSS, LADD-AH1, or LADD on day 7. Mice were treated with α-CD8 on day 6 and 8 when indicated. On day 11 in the TME. (*A*) Frequency of Treg in $CD45^+$ population. (*B*) CD8/Treg ratio. (*C*) iNOS production by TAMs. (*D*) CD206 expression by TAMs. (*E*) CT26 tumor-bearing mice (n = 4) were i.v. injected with LADD-AH1 on day 7. Lm per spleen, liver, or tumor were determined at 24 h, 72 h, and 7 d later. (*F* and *G*) Purified splenic $CD8^+$ T cells from LADD-AH1–treated or control CT26 tumor-bearing mice were cocultured with an untreated CT26 tumor suspension with or without 10 μg/mL IFNγ for 24 h. (*F*) iNOS production by TAMs. (*G*) CD206 expression by TAMs. (*H* and *I*) Conditions as *A–D*. (*H*) IFNγ level (picograms per milliliter) (*I*) TNFα level (picograms per milliliter) in supernatants of tumor. In scatter plots, each circle represents one mouse. All panels were analyzed by one-way ANOVA with Tukey's multiple comparisons test. $^*P < 0.05$, $^{**}P < 0.01$, $^{***}P < 0.001$, and $^{****}P < 0.0001$. Results are representative of at least two independent experiments.

Notably, LADD treatment also increased chemokines such as MCP3 and RANTES in the TME (*SI Appendix*, Fig. S6*C*).

LADD-Neo–induced $Adpgk^+$ $CD8^+$ T cells also infiltrated MC38 tumors (*SI Appendix*, Fig. S7 *A* and *B*), and resulted in an increased CD8/Treg ratio and iNOS production by TAMs (*SI Appendix*, Fig. S7 *C* and *D*). Together, these results show that LADD-Ag–induced IFNγ producing tumor-specific $CD8^+$ T cells infiltrate tumors, remodel the TME, and thus control tumor growth (*SI Appendix*, Fig. S8).

LADD-Ag Induces Effector Memory T Cells That Protect Against Tumor Rechallenge. We next characterized the level and function of tumor-specific $CD8^+$ T cells from CT26 tumor-bearing mice that were cured by LADD-AH1 treatment (survivors). Six weeks after LADD-AH1 treatment, a high percentage of $AH1^+CD8^+$ T cells persisted in survivors (Fig. 5*A*). These $AH1^+CD8^+$ T cells mostly expressed KLRG1 and T-bet but not Ki67 (Fig. 5 *B–D*), suggesting they were effector memory T cells. Furthermore, the $AH1^+KLRG^{hi}$T-bet^{hi} $CD8^+$ T cell population that persisted in the periphery were functional and completely protected mice against CT26 tumor rechallenge (Fig. 5*E* and *SI Appendix*, Fig. S9*A*). Notably, $CD8^+$ T cell depletion only partially impaired this ability (Fig. 5*E*). Significant levels of NK cells, iNOS-producing TAMs and AH1-specific $CD8^+$ T cells were detected in the TME of survivors 3 d after rechallenge with a very high dose of tumor cells (4×10^6) (*SI Appendix*, Fig. S9 *B–D*). Remarkably, about 60% of tumor-infiltrating $CD8^+$ T cells were AH1-specific in these mice (*SI Appendix*, Fig. S9*E*). Together, these data illustrate that LADD-AH1 treatment induced a large population of highly functional tumor-specific $CD8^+$ T cells that both repolarize the TME and elicit effective primary and secondary antitumor responses.

Discussion

The scientific rationale for the clinical advancement of Lm-based immunotherapies is in part due to observations in the mouse infection model where a single immunization with sublethal doses of WT Lm confers protection against lethal WT Lm challenge (26). Protection is entirely dependent upon potent bacterial-specific T cell immunity. While our previous investigations have demonstrated the antitumor potency of LADD-Ag (14), here we describe the immunologic correlates of this efficacy. We show that while LADD itself induced proinflammatory cytokines and some TME changes including decreased PD-1 expression on tumor-infiltrating $CD8^+$ T cells and an increased CD8/Treg ratio, these changes were not sufficient to confer antitumor efficacy. Instead, LADD-Ag primed high numbers of T-$bet^+KLRG1^{hi}PD\text{-}1^{lo}CD62L^-$ tumor-specific $CD8^+$ T cells in the spleen. This T cell population infiltrated the tumor, resulting in a TME profile measured at the transcriptional, protein, and cell population levels that differed significantly from LADD.

The lack of antitumor efficacy by LADD or LADD expressing an irrelevant antigen highlights the importance of expression of cognate tumor antigens. The magnitude of peripheral tumor-specific responses increased in tumor-bearing mice relative to naive animals upon LADD-Ag immunization. This result demonstrated that a robust tumor-specific immune response required tumor implantation and Ag presentation/priming, along with LADD-Ag immunization. Indeed, our adoptive transfer experiment showed that

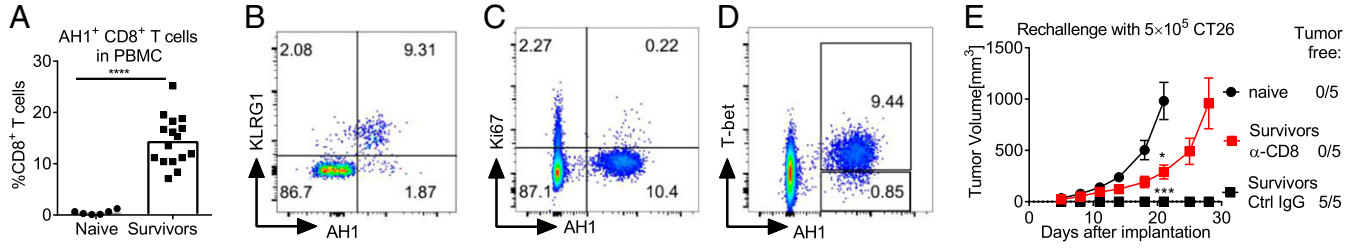

Fig. 5. LADD-AH1 induces memory effector $CD8^+$ T cells that protect survivors from CT26 rechallenge. Survivors and naive mice were reinoculated with CT26 in their left thoracic flanks. (*A–D*) Before reinoculation, (*A*) frequency of peripheral AH1 $tetramer^+$ of $CD8^+$ T cells, (*B–D*) Representative staining of AH1 tetramer and (*B*) KLRG1, (*C*) Ki67, or (*D*) T-bet of peripheral $CD8^+$ T cells in survivors. (*E*) S.c. growth of 5×10^5 CT26 in naive mice (n = 5) and survivors treated with control IgG or α-CD8. Tumor volumes ±SEM are shown. In scatter plots, each circle represents one mouse. FACS plots show representative analysis for one mouse per group. *A* was analyzed by Mann–Whitney *U* tests. *E* was analyzed by two-way ANOVA. $^*P < 0.05$ and $^{****}P < 0.0001$. Results are representative of at least two independent experiments.

tumor implantation itself primed AH1$^+$CD8$^+$ T cells, which could be amplified by LADD-AH1 immunization (Fig. 2*J*). These data are consistent with previous observations that AH1 is a weak agonist for its cognate T cell receptor [K_D = 5.7 μM, $t_{1/2}$ (s) = 2] (27) and the dominant target for CT26-specific CTL responses (15). In contrast, LLO responses were comparable in tumor-bearing and naive mice because LLO is strongly immunogenic and is presented to CD4$^+$ and CD8$^+$ T cells at pM and nM levels (28).

Tumor growth can proceed unabated despite abundant tumor-specific T cells in the TME (Fig. 3*D*), indicating that these T cells are dysfunctional. Rapid induction of dysfunctional tumor-specific T cells occurs through continuous antigen encounter in an immunosuppressive TME (2). It is well-established that microbial infection can induce protective pathogen-specific T cells (9). In this study, we utilized attenuated Lm to generate functional cytotoxic CD8$^+$ T effector cells that overcome the immunosuppressive TME and promote tumor rejection. LADD-Ag delivers antigens into the cytoplasm of infected cells such as dendritic cells (DCs) for processing and presentation on MHC molecules, which provides a sustained source of tumor antigen and innate immune stimulation. In this context, tumor-specific T cells were amplified where tumor antigen was presented on activated DCs. The phenotypic CX3CR1$^+$CD62L$^-$KLRG1$^+$PD-1^{lo} profile of LADD-Ag–induced tumor-specific CD8$^+$ T cells resembled that of cytolytic pathogen-specific effector cells (11, 29). The phenotype of LADD-Ag induced CD8$^+$ T cells allowed us to distinguish them from resident tumor-specific T cells. Transcriptome analysis further revealed distinct functional signatures of tumor-specific T cells resulting from LADD-based immunotherapy. Tumor-specific T cells induced in the inflammatory context were less exhausted, produced IFNγ, controlled tumor growth, and established long-term memory.

Both antigens and adjuvants remain the focus of questions surrounding the optimal design of cancer vaccines. Viral antigens and neoantigens are considered ideal targets because of the lack of central tolerance (8). The preclinical potency of LADD expressing the viral antigens AH1 and E7 highlights the therapeutic potential of targeting viral antigens. Indeed, numerous therapeutic vaccination strategies against E7 have been developed for the treatment of cervical cancer and HPV-associated disease (30). Moreover, the strength of vaccine-induced T cell immune responses correlates with the clinical response (31). Interestingly, human endogenous retroviral antigens are emerging as novel immunotherapy targets (32). Notably, gp70 levels are strikingly high in murine tumor cell lines (16), and the gp70-derived AH1 epitope is highly immunodominant, which could explain both LADD-AH1 antitumor efficacy and the lack of epitope spreading against other known CT26 antigens. In addition to viral antigens, LADD-Neo can elicit neoantigen-specific CD8$^+$ T cells and TME changes in a preclinical mouse model, which provides rationale for LADD treatment targeting neoantigens. We recently initiated a clinical trial targeting neoantigens in patients with microsatellite stable colorectal cancer (NCT03189030). The possibility of developing antigen-loss variants is limited by designing LADD expressing multiple neoepitopes that can activate T cells against a variety of antigens. Many platforms are currently used for cancer vaccine development. Compared with the other platforms we tested, LADD appears to be an optimal vehicle for active immunotherapy in mice. Further experiments are required to fully understand its superior activity in preclinical models.

Materials and Methods

LADD-Ag strains, cells, antibodies, and other reagents used in this study are described in *SI Appendix*. Detailed information on immunization, in vivo tumor experiments, antibody staining and flow cytometry analysis, IFNγ ELISpot and ICS assays, isolation of CD8$^+$ T cells and RNA-Seq, adoptive transfer of CD8$^+$ T cells, luminex, IHC staining and histological analysis of CD8 infiltration, LADD biodistribution studies, and statistics can be found in *SI Appendix*. This study was performed according to protocols approved by the Institutional Animal Use Committee of Aduro Biotech.

ACKNOWLEDGMENTS. We thank Weiqun Liu, Yusup Chang, and Bruna Hedberg for support of the study; Hector Nolla and Alma Valeros at University of California, Berkeley for help with cell sorting; and Leticia Corrales for preparing the Graphical abstract. We are grateful to David Raulet and Erin Benanti for helpful comments. We thank the research department at Aduro Biotech for useful discussion and comments on the manuscript.

1. Sharma P, Hu-Lieskovan S, Wargo JA, Ribas A (2017) Primary, adaptive, and acquired resistance to cancer immunotherapy. *Cell* 168:707–723.
2. Schietinger A, et al. (2016) Tumor-specific T cell dysfunction is a dynamic antigen-driven differentiation program initiated early during tumorigenesis. *Immunity* 45:389–401.
3. Chanmee T, Ontong P, Konno K, Itano N (2014) Tumor-associated macrophages as major players in the tumor microenvironment. *Cancers (Basel)* 6:1670–1690.
4. Stein M, Keshav S, Harris N, Gordon S (1992) Interleukin 4 potently enhances murine macrophage mannose receptor activity: A marker of alternative immunologic macrophage activation. *J Exp Med* 176:287–292.
5. Dalton DK, et al. (1993) Multiple defects of immune cell function in mice with disrupted interferon-gamma genes. *Science* 259:1739–1742.
6. Khalil DN, Smith EL, Brentjens RJ, Wolchok JD (2016) The future of cancer treatment: Immunomodulation, CARs and combination immunotherapy. *Nat Rev Clin Oncol* 13:273–290.
7. Coffman RL, Sher A, Seder RA (2010) Vaccine adjuvants: Putting innate immunity to work. *Immunity* 33:492–503.
8. Melief CJ, van Hall T, Arens R, Ossendorp F, van der Burg SH (2015) Therapeutic cancer vaccines. *J Clin Invest* 125:3401–3412.
9. Harty JT, Tvinnereim AR, White DW (2000) CD8+ T cell effector mechanisms in resistance to infection. *Annu Rev Immunol* 18:275–308.
10. McMahon CW, et al. (2002) Viral and bacterial infections induce expression of multiple NK cell receptors in responding CD8(+) T cells. *J Immunol* 169:1444–1452.
11. Olson JA, McDonald-Hyman C, Jameson SC, Hamilton SE (2013) Effector-like CD8$^+$ T cells in the memory population mediate potent protective immunity. *Immunity* 38:1250–1260.
12. Glomski IJ, Decatur AL, Portnoy DA (2003) Listeria monocytogenes mutants that fail to compartmentalize listerolysin O activity are cytotoxic, avirulent, and unable to evade host extracellular defenses. *Infect Immun* 71:6754–6765.
13. Cossart P, Pizarro-Cerdá J, Lecuit M (2003) Invasion of mammalian cells by Listeria monocytogenes: Functional mimicry to subvert cellular functions. *Trends Cell Biol* 13:23–31.
14. Brockstedt DG, et al. (2004) Listeria-based cancer vaccines that segregate immunogenicity from toxicity. *Proc Natl Acad Sci USA* 101:13832–13837.
15. Huang AY, et al. (1996) The immunodominant major histocompatibility complex class I-restricted antigen of a murine colon tumor derives from an endogenous retroviral gene product. *Proc Natl Acad Sci USA* 93:9730–9735.
16. Scrimieri F, et al. (2013) Murine leukemia virus envelope gp70 is a shared biomarker for the high-sensitivity quantification of murine tumor burden. *OncoImmunology* 2: e26889.
17. Li J, Sun Y, Garen A (2002) Immunization and immunotherapy for cancers involving infection by a human papillomavirus in a mouse model. *Proc Natl Acad Sci USA* 99:16232–16236.
18. Ott PA, et al. (2017) An immunogenic personal neoantigen vaccine for patients with melanoma. *Nature* 547:217–221.
19. Sahin U, et al. (2017) Personalized RNA mutanome vaccines mobilize poly-specific therapeutic immunity against cancer. *Nature* 547:222–226.
20. Yadav M, et al. (2014) Predicting immunogenic tumour mutations by combining mass spectrometry and exome sequencing. *Nature* 515:572–576.
21. Kreiter S, et al. (2015) Mutant MHC class II epitopes drive therapeutic immune responses to cancer. *Nature* 520:692–696.
22. Schwab SR, Cyster JG (2007) Finding a way out: Lymphocyte egress from lymphoid organs. *Nat Immunol* 8:1295–1301.
23. Lizotte PH, et al. (2014) Attenuated *Listeria monocytogenes* reprograms M2-polarized tumor-associated macrophages in ovarian cancer leading to iNOS-mediated tumor cell lysis. *OncoImmunology* 3:e28926.
24. Sawanobori Y, et al. (2008) Chemokine-mediated rapid turnover of myeloid-derived suppressor cells in tumor-bearing mice. *Blood* 111:5457–5466.
25. Priceman SJ, et al. (2010) Targeting distinct tumor-infiltrating myeloid cells by inhibiting CSF-1 receptor: Combating tumor evasion of antiangiogenic therapy. *Blood* 115:1461–1471.
26. MacKaness GB (1964) The immunological basis of acquired cellular resistance. *J Exp Med* 120:105–120.
27. Slansky JE, et al. (2000) Enhanced antigen-specific antitumor immunity with altered peptide ligands that stabilize the MHC-peptide-TCR complex. *Immunity* 13:529–538.
28. Carrero JA, Vivanco-Cid H, Unanue ER (2012) Listeriolysin o is strongly immunogenic independently of its cytotoxic activity. *PLoS One* 7:e32310.
29. Böttcher JP, et al. (2015) Functional classification of memory CD8(+) T cells by CX3CR1 expression. *Nat Commun* 6:8306.
30. Lee SJ, Yang A, Wu TC, Hung CF (2016) Immunotherapy for human papillomavirus-associated disease and cervical cancer: Review of clinical and translational research. *J Gynecol Oncol* 27:e51.
31. Welters MJ, et al. (2010) Success or failure of vaccination for HPV16-positive vulvar lesions correlates with kinetics and phenotype of induced T-cell responses. *Proc Natl Acad Sci USA* 107:11895–11899.
32. Gonzalez-Cao M, et al. (2016) Human endogenous retroviruses and cancer. *Cancer Biol Med* 13:483–488.